



University of Bahrain
**Journal of the Association of Arab Universities for
 Basic and Applied Sciences**

www.elsevier.com/locate/jaaubas
www.sciencedirect.com



Assessment of adsorption kinetics for removal potential of Crystal Violet dye from aqueous solutions using Moroccan pyrophyllite

Youssef Miyah ^{a,b,*}, Anissa Lahrichi ^b, Meryem Idrissi ^a, Saïd Boujraf ^c,
 Hasnae Taouda ^d, Farid Zerrouq ^a

^a *Laboratory of Catalysis, Materials and Environment, School of Technology, University Sidi Mohammed Ben Abdellah, Fez, Morocco*

^b *Laboratory of Biochemistry, Faculty of Medicine and Pharmacy, University Sidi Mohammed Ben Abdellah, Fez, Morocco*

^c *Laboratory of Biophysics and Clinical MRI Methods, Faculty of Medicine and Pharmacy, University Sidi Mohammed Ben Abdellah, Fez, Morocco*

^d *Laboratory of Bioactive Molecules, Faculty of Science and Technology, University Sidi Mohammed Ben Abdellah, Fez, Morocco*

Received 7 September 2015; revised 1 June 2016; accepted 5 June 2016

KEYWORDS

Adsorption;
 Pyrophyllite;
 Isotherm;
 Modeling;
 Regenerated

Abstract This study involves the adsorption of Crystal Violet (CV) dye adsorbed from solution on the pyrophyllite's surface. The batch technique was used under a variety of conditions to produce quantitative adsorption, namely amount of adsorbent, dye concentration, contact time, pH solution and temperature. The maximum adsorption capacity of Crystal Violet on pyrophyllite was 9.58 mg/g for 10 mg/L of CV concentration, pH = 6.8 at a temperature 20 °C and 1 g/L of adsorbent. This study of adsorption kinetics was carried out within framework of three models: intraparticle diffusion, pseudo-first order and pseudo-second order. The experimental isotherm data were analyzed using Langmuir and Freundlich models. Different thermodynamic parameters have shown spontaneous reaction with endothermic nature (The estimated value for ΔG was -7.64 kJ/mol at 293 K). Various techniques for characterizing the adsorbent were applied including X-ray diffraction (XRD), X-ray fluorescence spectroscopy (XRF), scanning electron microscopy (SEM) and transmission electron microscopy (TEM) coupled by energy dispersive X-ray spectroscopy (EDX). In addition, the regenerated adsorbents technique was reused several times; this demonstrated an economical aspect of using pyrophyllite which underlines the re-use importance considering the material capacity to regenerate.

© 2016 University of Bahrain. Production and hosting by Elsevier B.V. This is an open access article under the CC BY-NC-ND license (<http://creativecommons.org/licenses/by-nc-nd/4.0/>).

* Corresponding author at: Laboratory of Catalysis, Materials and Environment, High School of Technology, University Sidi Mohammed Ben Abdellah, Fez, Morocco. Tel.: +212 0645832284.

E-mail addresses: youssef.miyah@gmail.com, youssef.miyah@usmba.ac.ma (Y. Miyah).

Peer review under responsibility of University of Bahrain.

<http://dx.doi.org/10.1016/j.jaubas.2016.06.001>

1815-3852 © 2016 University of Bahrain. Production and hosting by Elsevier B.V.

This is an open access article under the CC BY-NC-ND license (<http://creativecommons.org/licenses/by-nc-nd/4.0/>).

1. Introduction

Recently, dyeing has allowed various synthetic dye techniques in wastewater of industries such as textiles (Gupta and Suhas, 2009; Mohamad Amran et al., 2011). In this respect, many industrial processes use toxic chemicals to finish manufactured products. Thus, unused part of these chemicals gets away into the environment as industrial waste; this affects rivers and the quality of water. Indeed, very low toxin concentrations might be highly visible and would significantly affect photosynthetic activity of aquatic life due to reduced light penetration (Wojciech et al., 2015). Additionally, the cationic dyes are more toxic compared to anionic ones (Hao et al., 2000), they might cause allergies and suffocation because of easy interactions between cationic dyes and the negatively charged cell membrane surfaces (Li, 2010). As a starting point, Crystal Violet (CV) is a water-soluble cationic dye belonging to the class of triarylmethane dyes; they are widely used in textile industries for dyeing cotton, acrylic, nylon, wool, leather, paper, plastics and silk (Mittal et al., 2010). Further, it's a carcinogenic that has been classified among the recalcitrant molecules since it is poorly metabolized by microbial flora; it is not only biodegradable but it might persist in environmental medium as well (Haik et al., 2010; Mohamad Amran et al., 2011). Hence, worldwide environmental scientists have faced this threat by developing cost effective and efficient technologies for CV treatment (Mittal et al., 2010; Mohamad Amran et al., 2011; Sivashankar et al., 2014).

Therefore, evolving a sustainable competitive method for effluent management for the dyeing industry has been a crucial task while targeting the environment protection (Ellouze et al., 2012). Conventional physico-chemical processes for dye removal from wastewater include oxidation, photochemical degradation, reverse osmosis, membrane separation, coagulation and adsorption (El Haddad et al., 2013; Gupta and Suhas, 2009; Idrissi et al., 2014; Mahmoodi et al., 2011; Ollis et al., 2015). The latter is one of the most effective methods that has been successfully adopted for the removal of wastewater color (Mustafa et al., 2014).

The activated carbon is a largely used adsorbent seeing that it has a high adsorption capacity of organic materials (Gupta and Suhas, 2009; Njoku et al., 2014). However, this adsorbent is very expensive and remains difficult to regenerate. The investigation of other effective and less expensive adsorbents demonstrated peat soil capability, hydroxyapatite, chitin-chitosan and clay minerals (Barka et al., 2011; Gupta and Suhas, 2009; Mehmet et al., 2009; Zhiguo et al., 2014). The latter was widely studied since it is cost effective, accessible and available.

Recently, the application of pyrophyllite on wastewater treatment has interested the scientific community. Publications have reported the pyrophyllite potential for removal of heavy metal ions and dyes (Sheng et al., 2009).

In this work, our target is to study the basic dye Crystal Violet adsorption on pyrophyllite. For this reason, various experimental parameters were analyzed: amount of adsorbent, initial concentration while coloring, contact time, pH solution and temperature. The adsorption capacities were given using the Langmuir and Freundlich isotherms. While the adsorption kinetics of the Crystal Violet was studied using the intraparticle

diffusion equations, the pseudo-first order and the pseudo-second order models.

2. Materials and methods

2.1. Preparation of adsorbent

The rough pyrophyllite PY used in this work has been taken from a natural basin in the south of Morocco; it was crushed and filtered to obtain fractions $< 80 \mu\text{m}$ then dried at 105°C during 24 h.

2.2. Preparation of adsorbate

The adsorbate, Crystal Violet (CV) dye (chemical formula = $\text{C}_{25}\text{H}_{30}\text{N}_3\text{Cl}$, molecular weight = 407.98 g/mol, solubility in water 16 g/L at 25°C) was obtained from Sigma-Aldrich (purity = 99%). The structure of Crystal Violet is illustrated in Fig. 1. Stock solution was prepared by dissolving accurately the weighed dye in ultrapure water to obtain a concentration of 1000 mg/L.

2.3. Determination of zero point charge

The zero point charge pH (pH_{ZPC}) of PY adsorbent was measured using pH drift method applied by researchers El Haddad et al. (2013). In this fact, pH_{ZPC} of adsorbent was determined by adding 20 mL of NaCl ($5 \cdot 10^{-2}$ mol/L) to several 50 mL beaker of polystyrene. A range of initial pH (pH_i) values of NaCl solutions were adjusted from 2 to 12 by adding drops of HCl and NaOH (0.1 mol/L). The total solution volume in each flask was brought to exactly 30 mL by further addition $5 \cdot 10^{-2}$ mol/L of NaCl solution. pH_i values of solutions were then accurately noted and 50 mg of each adsorbent were added to each flask, which was securely and immediately capped. Suspensions were shaken at 298 K; this allowed to equilibrate for 48 h. Suspensions were filtered using a membrane filter from pore diameter of $0.45 \mu\text{m}$ and the final pH (pH_f) values of the supernatant liquid were recorded.

The value of pH_{ZPC} is the point where the curve of ΔpH ($\text{pH}_f - \text{pH}_i$) versus pH_i crosses the line equal to zero while pH_{ZPC} is determined by the intersection point of curve. Measured pH was down by pH-Meter (Hach sension 2 pH ISE meter).

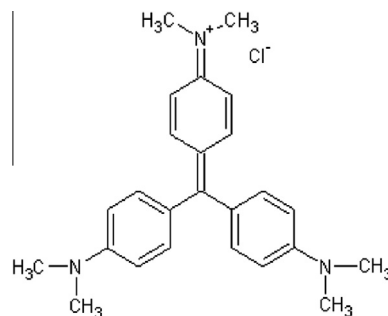


Figure 1 Structure of Crystal Violet (CV).

2.4. Adsorption procedure

Adsorbent PY was characterized by various analysis methods: XDR (Panalytical company), Cu radiation K_{α} ($\lambda = 1.54060$ nm), functioning to 40 kV and 30 mA. The data were collected with $2\theta = 10\text{--}80^{\circ}$. XRF used a sequential spectrometer with a channel of measurement based on one goniometry covering the complete range of measurement from B to U (AXIOS PANALYTICAL). FTIR technique used a range sweeping wavelength $400\text{--}7500\text{ cm}^{-1}$ (BRUKER Vertex70). SEM-EDX analysis equipped with probe EDX for microanalysis of surfaces (Quanta 200 FEI) and TEM analysis with an enlarging from 150 to 500,000 times (FEI TECNAI G2).

Pyrophyllite was tested for reagent coloring adsorption of Crystal Violet dye starting from aqueous solutions with room temperature using batch processing technique (Miyah et al., 2015). Adsorption measurements were carried out by mixing various pyrophyllite quantities for eliminating Crystal Violet dye potential in a series of beakers containing 200 mL of solution colored by different pHs using heating with numerical control and a magnetic stirrer (Stuart). Dye solutions were prepared using ultrapure water (MILLIPORE, direct-Q, UV3 with Pump) to prevent and minimize any possible interferences. Specimens were accomplished using a syringe filter of $0.45\ \mu\text{m}$ diameter (Minisart, sartorium stedim biotech). The effect of several variables such as the pyrophyllite amount (0.5–2 g/L), the contact time (0–120 min), the initial concentration while coloring (5–20 mg/L), the pH (4–12) and the temperature of the solution (20–50 °C) were all studied.

The pH solution was adjusted by adding drops of HCl and NaOH (0.1 mol/L). After 20 min, the balance was established. At the end of adsorption experiments, the dye concentration was given by measuring the solution absorbance at $\lambda = 588$ nm using a UV–visible spectrophotometer (Jasco V530). All experiments were carried-out in triplicate and the medium values are presented.

The amount of equilibrium adsorption q_e (mg/g) was calculated using the formula:

$$q_e = \frac{C_0 - C_e}{W} V \quad (1)$$

The dye removal percentage can be calculated as follows:

$$\% \text{dye removal} = \frac{C_0 - C_e}{C_0} \times 100 \quad (2)$$

where C_0 and C_e (mg/L) are respectively the liquid concentrations of initial and at equilibrium dye, V is the volume of the solution (L) and W is the mass of adsorbent (g).

3. Results and discussion

3.1. Characterization of adsorbents

Typical chemical compositions analysis have been realized by XRF of pyrophyllite sample in percentages were as follows: SiO_2 (63.59%), Al_2O_3 (28.453%), L.O.I (loss on ignition) (5.43%), Fe_2O_3 (0.93%), Na_2O (0.56%), K_2O (0.32%), MgO (0.254%), SO_3 (0.123%), TiO_2 (0.119%), P_2O_5 (0.114%),

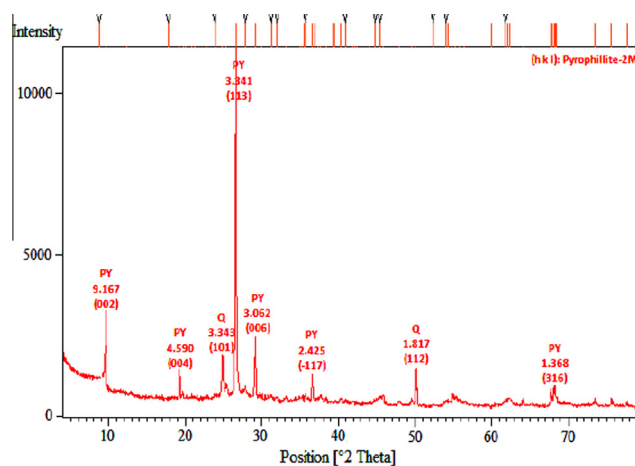


Figure 2 XRD pattern of pyrophyllite (PY).

and CaO (0.107%). Pyrophyllite sample contained a higher molar ratio of $\text{SiO}_2/\text{Al}_2\text{O}_3$ (2.23). The chemical analysis indicated that our pyrophyllite samples contained 95% of pure pyrophyllite.

Consistently, XRD patterns obtained from the mineral revealed that ore sample mainly contained pyrophyllite and quartz. Fig. 2 shows the peaks at 9.167 (002), 4.590 (004), 3.341 (113), 3.062 (006), 2.425 (–117), 1.368 (316), and peaks at 3.343 (101), 1.817 (112), which are characteristic peaks for pyrophyllite and quartz respectively. Obtained results from XRD peaks in our study were confirmed by several researchers finding similar results for pyrophyllite peaks (Zhang et al., 2015).

Our samples were analyzed by scanning electron microscopy (SEM) coupled by energy dispersive X-ray spectroscopy (EDX) and transmission electron microscopy (TEM). The application of these techniques made it possible to visualize the surface morphology of adsorbents. The images (3a) of microscopy SEM (Fig. 3) show a porous aspect which facilitates materials adsorption. In addition, spectrum EDX (3b) shows the presence of elements which were previously quoted to know Al, Si, Na, Mg, Fe and Ca. This result confirms the validity of the X-ray fluorescence analysis. TEM examination of pyrophyllite that was presented in the same Fig. 3, images (3c and 3d) shows that the lamellate of laminated form is distributed well; it is noticed that each leaf consists of a poisoned aluminum octahedral layer between two tetrahedral layers of silica (Guanghui et al., 2014).

3.2. Effect of contact time and Crystal Violet's dye concentration

The study of Crystal Violet's adsorption on PY adsorbent in solution implies: determination of contact time corresponding to the balance of adsorption/desorption or a state of support saturation balance by the substrate. The adsorption experiments for evaluating the contact time effect on the adsorption of Crystal Violet on the adsorbent selected were carried out on Crystal Violet solutions in the initial concentration range varying from 5 to 20 mg/L and at a temperature of 20 °C for a duration of 120 min. The determination of the contact time

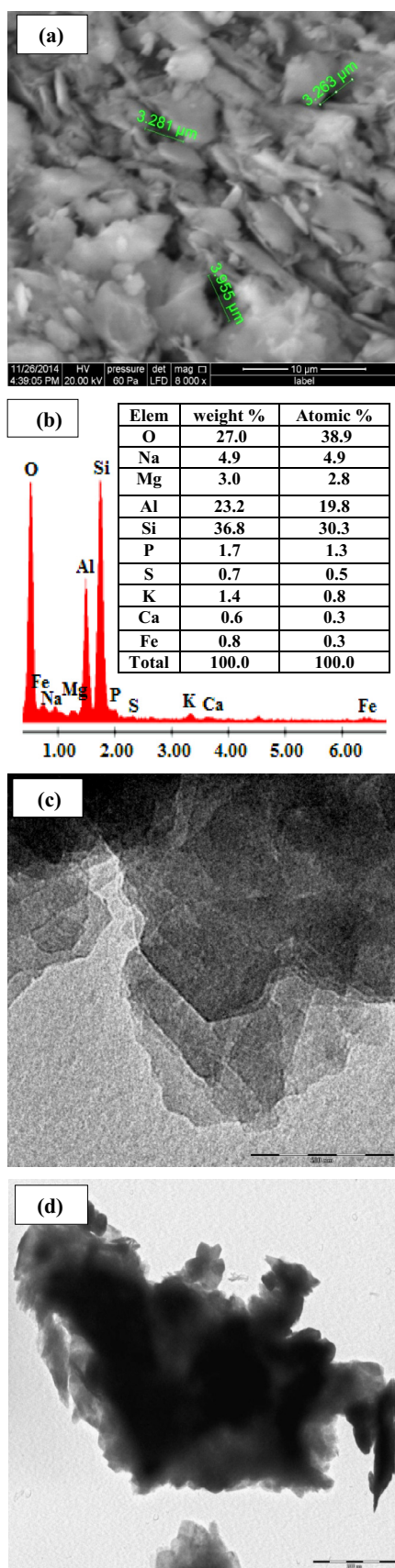


Figure 3 SEM microscopy coupled by EDAX, for PY (3a and 3b), and TEM microscopy (3c and 3d).

corresponding to adsorption balance has allowed establishing the adsorption isotherms. The knowledge of this time is essential for calculating the maximum adsorption capacity and for identification of the adsorption type which can occur into mono or multi-layer (Miyah et al., 2015). Results presented in Fig. 4 show that the adsorbed quantity of Crystal Violet (CV) increases quickly in the first 15 min and remains constant after 20 min indicating a balance state. Indeed, some sites are difficult to occupy; that is due to the repulsion between Crystal Violet molecules adsorbed on the solid surface and those of the aqueous medium this leads to a saturation of adsorbent sites and therefore a reach of an equilibrium state after 20 min. One can notice that the initial concentration of the CV does not have any significant effect over equilibrium time, but it is of paramount effect on the adsorption capacity of the support. The adsorbed quantity for PY adsorbent increases with Crystal Violet initial concentration rise. This can be explained by the presence of a big molecule number which will diffuse toward sites of the adsorbent surface and consequently partial adsorption depends on the initial concentration.

3.3. Effect of adsorbent amount

The study of the pyrophyllite mass influence on the adsorbed quantity of Crystal Violet according to time (q_t) and on eliminated percentage of dye at equilibrium was represented in Fig. 5. The adsorption percentage increased with adsorbent's dosage rise, but the amount of adsorbed dye per adsorbent unit mass decreased with a rise in adsorbent amount from 0.5 to 2 g/L. As the adsorbent amount increases, the number of active sides available for adsorption increases as well; thus, the percentage of removal also increases since all active sides may not be available during adsorption due to overlapping between active sides themselves and the adsorbed amount (mg/g) of adsorbent decreases. As a result, the percentage of the dye's adsorption increased with the adsorbent amount and reached an equilibrium value after a certain adsorbent dosage (1–1.5 g/L) for most adsorbents.

3.4. Effect of pH

The behavior of CV adsorption on PY adsorbent was studied on a broad range of pH 4–12. Fig. 6 shows a light increase in the adsorbed quantity of dye by pyrophyllite with the increase in pH solution. The zero point load (ZPC) of pyrophyllite PY is 7.3. This behavior is mostly due to the fact that the PY surface is negatively charged when $\text{pH} > \text{ZPC}$, which supports the adsorption of Crystal Violet's cationic dye. On the other hand, for values of $\text{pH} < \text{ZPC}$, the PY surface is charged positively and thus likely to push back cations of dye. The more pH decreases the more the number of negatively charged sites falls and the number of positively charged sites increases (Weng and Pan, 2007).

The analysis of these results shows that the adsorbed quantity of Crystal Violet on pyrophyllite increases with the increased pH solution.

3.5. Effect of temperature

The temperature is a strongly significant parameter in the adsorption process. It is important to include the influence

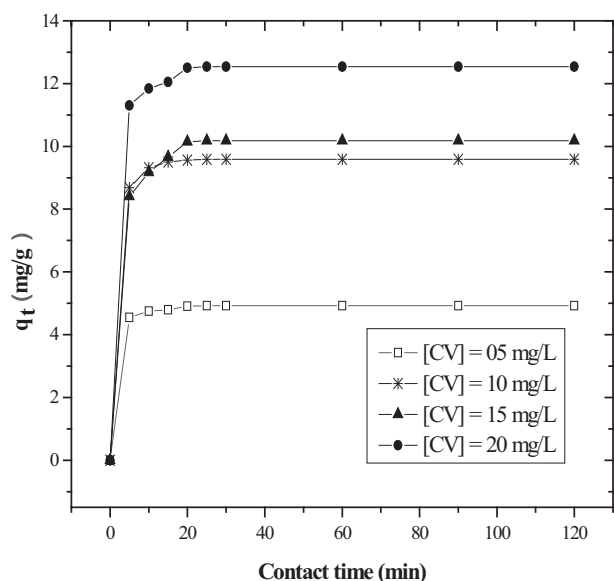


Figure 4 Effect of contact time and CV dye concentration. Interval of initial concentration (5–20 mg/L), adsorbent amount: $W = 0.2$ g, $V = 200$ mL, $\text{pH} = 6.8$, $T = 20$ °C, and agitation time 120 min.

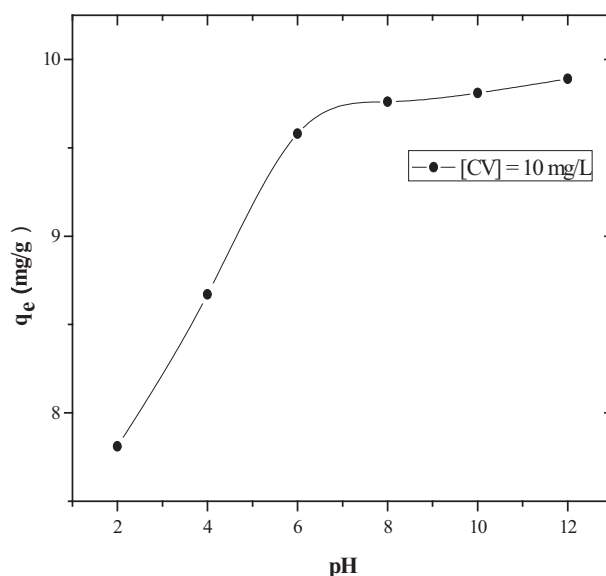


Figure 6 Effect of pH on adsorbed quantity of CV onto PY. Interval of pH (4–12), Initial dye concentration 10 mg/L. Adsorbent amount: $W = 0.2$ mg, $V = 200$ mL, $T = 20$ °C, and agitation time 120 min.

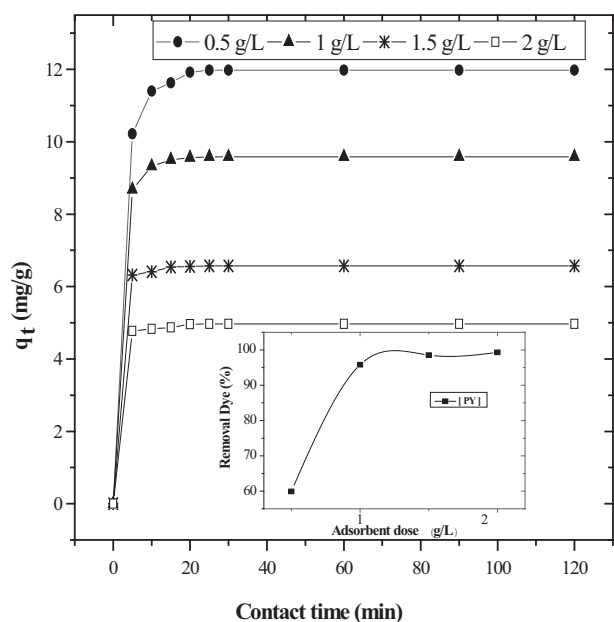


Figure 5 Effect of adsorbent amount on both adsorption quantity and dye removal of CV. Interval of adsorbent amount (0.5–2 g/L), Initial dye concentration 10 mg/L, $V = 200$ mL, $\text{pH} = 6.8$, $T = 20$ °C, and agitation time 120 min.

of this parameter during the Crystal Violet adsorption on PY. In this work, we have studied the temperature effect on the Crystal Violet's adsorbed quantity in the range of 20–50 °C (Fig. 7). The adsorbed quantity of Crystal Violet with balance q_e (mg/g) on the adsorbent increases with temperature in the study range and the adsorption time required

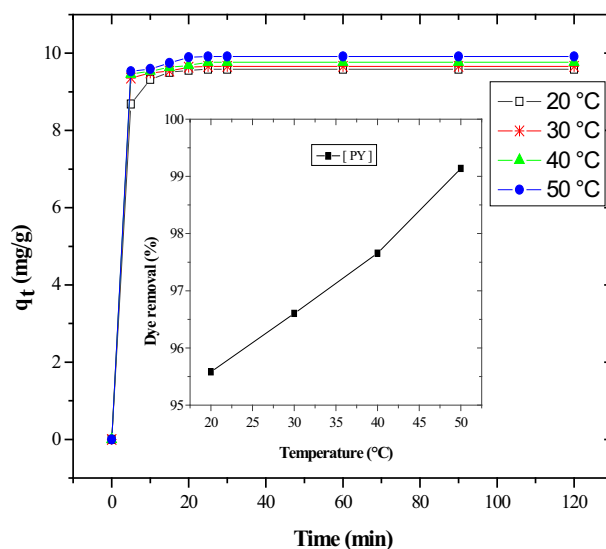


Figure 7 Effect of temperature on both adsorbed quantity and dye removal of CV. Interval of temperature (20–50 °C), Initial dye concentration 10 mg/L. Adsorbent amount: $W = 0.2$ mg, $V = 200$ mL, $\text{pH} = 6.8$, $T = 20$ °C, and agitation time 120 min.

reaching balance decreases with the increase of temperature which means that the adsorption process is endothermic. Singh et al. (2011) mentioned that the number of binding sites for dye molecules on the adsorbent surface may be increased by the increased temperature. Güzel et al. (2015) showed that this may be illustrated by the fact that the increased temperature adds power to the adsorbate molecule spread rate across the external limit layer and the internal pores of the adsorbent

particles as a result of reduced solution's viscosity. In addition, the mobility of adsorbate molecules also increases with temperature (Almeida et al., 2009) facilitating the formation of surface monolayer's. Generally, the temperature elevation promotes adsorption.

3.6. Adsorption kinetics

Several models can be used to express the controlling mechanism of adsorption process such as mass transfer and chemical reaction. The intraparticle diffusion, pseudo-first order and pseudo-second order models that were used to test the fit of experimental data of dye adsorption by PY on the kinetics equations proposed by various authors (Lagergren, 1898; Weber and Morris, 1963). The contribution of the intraparticle diffusion mechanism can be tested by applying the Weber and Morris (1963) equation:

$$q_t = K_p t^{\frac{1}{2}} + I \quad (3)$$

where q_t is the amount of solute on the surface of the adsorbent at time t (mg/g), K_p is the intraparticle rate constant (mg/g min^{1/2}), t is the time (min) and I (mg/g) is a constant that gives an idea about the thickness of the boundary layer.

According to the intraparticle equation, the plot of q_t versus $t^{1/2}$ should be linear. If the plots are not totally linear, and more so does not pass through the origin, then intraparticle diffusion could not be the only mechanism involved (Weber and Morris, 1963).

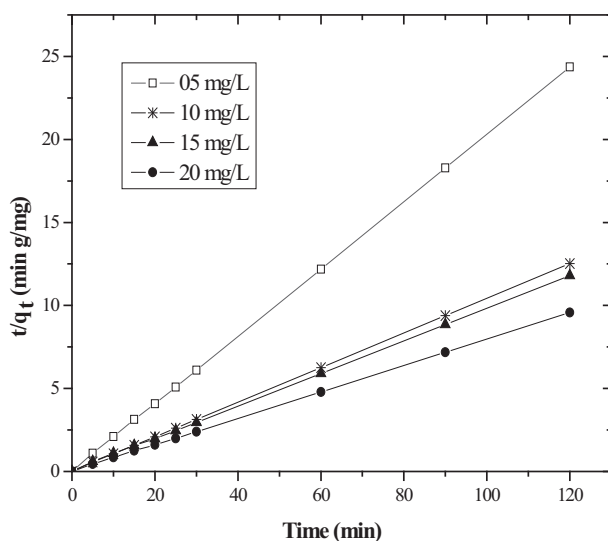


Figure 8 Pseudo-second order model of adsorption kinetics.

The kinetics model of pseudo-first order is mostly adapted for the weakest concentrations of aqueous solution. This model is presented by the relation of Lagergren based on the adsorbed quantity; it is the first equation speed established to describe the adsorption kinetics in a liquid/solid system. This model of pseudo-first order is represented by the following relation (Ru-Ling et al., 2014):

$$\ln(q_e - q_t) = \ln q_e - K_1 t \quad (4)$$

where K_1 is the constant speed of adsorption of the pseudo-first order model (min⁻¹), a straight line of $\ln(q_e - q_t)$ versus t indicates the application of pseudo-first order kinetics model. In a true pseudo-first order process, $\ln q_e$ should be equal to the interception of an $\ln(q_e - q_t)$ plot against t .

The pseudo-first order considers the adsorption rate of occupation sites to be proportional to the number of unoccupied sites. The pseudo-second order equation (Talal, 2014), another equation used for kinetics analysis, is based on the adsorption equilibrium capacity that may be expressed in the following form:

$$\frac{t}{q_t} = \frac{1}{K_2 q_e^2} + \frac{t}{q_e} \quad (5)$$

where K_2 is the constant speed of adsorption model of pseudo-second order (g/mg min⁻¹); if this equation is checked, by tracing t/q_t according to t , we must obtain a line of slope $1/q_e$ and ordinate in the beginning equal to $1/(K_2 q_e^2)$.

The adsorption kinetics modeling of CV on PY adsorbent by pseudo-second order model is presented in Fig. 8.

The three kinetic model parameters are gathered in Table 1, which also presents the correlation coefficients and the adsorbed quantity. From these results, it is noted that in case of intraparticle diffusion kinetics model and pseudo-first order the quantity adsorbed with balance determined in experiments is different from that calculated. On the other hand, the adsorbed quantity with balance, determined in experiments, is closer to the calculated value using the kinetics model of the pseudo-second order. This model is applied to systems in case of adsorbing/adsorbed studied considering the obtained values of R^2 coefficients, which are very close to the unit.

3.7. Adsorption isotherms

The Langmuir model is based on chemical interactions between solute molecules and adsorbent. According to this model, the adsorption of molecules occurs in a single layer (forming a molecular monolayer). This localized adsorption on specific sites can contain only one molecule per site (Langmuir, 1916). The mathematical expression is:

Table 1 Comparison between the intraparticle diffusion model, pseudo-first order and pseudo-second order adsorption constant rate, calculated and experimental q_e values for different initial CV concentrations.

| Dye concentration (mg/L) | $(q_e)_{\text{exp}}$ | Intraparticle diffusion | | | Pseudo-first order | | | Pseudo-second order | | |
|--------------------------|----------------------|-------------------------|-------|---------|----------------------|-------|---------|----------------------|-------|---------|
| | | K_p | I | R_I^2 | $(q_e)_{\text{cal}}$ | K_1 | R_F^2 | $(q_e)_{\text{cal}}$ | K_2 | R_S^2 |
| 05 | 4.92 | 0.13 | 4.21 | 0.951 | 1.13 | 0.08 | 0.860 | 4.93 | 0.94 | 0.999 |
| 10 | 9.58 | 0.39 | 7.91 | 0.884 | 1.61 | 0.10 | 0.999 | 9.60 | 0.60 | 0.999 |
| 15 | 10.17 | 0.67 | 6.99 | 0.968 | 2.78 | 0.11 | 0.843 | 10.24 | 0.19 | 0.999 |
| 20 | 12.54 | 0.46 | 10.31 | 0.969 | 2.06 | 0.09 | 0.819 | 12.58 | 0.25 | 0.999 |

Table 2 Isotherm constants for dye adsorption at different temperatures onto PY.

| Temperature (°C) | Langmuir isotherm model | | | Freundlich isotherm model | | |
|------------------|-------------------------|-------|---------|---------------------------|-------|---------|
| | q_L | K_L | R_L^2 | K_F | n_F | R_F^2 |
| 20 | 12.19 | 4.315 | 0.981 | 8.75 | 5.91 | 0.816 |
| 30 | 12.82 | 4.333 | 0.980 | 9.14 | 5.78 | 0.823 |
| 40 | 13.51 | 4.933 | 0.982 | 9.68 | 5.61 | 0.805 |
| 50 | 13.88 | 7.200 | 0.994 | 10.40 | 6.49 | 0.685 |

Table 3 Dimensionless separation factor R_L .

| [CV] (mg/L) | Temperature (K) | | | |
|-------------|-----------------|-------|-------|-------|
| | 293 | 303 | 313 | 323 |
| 5 | 0.044 | 0.044 | 0.038 | 0.027 |
| 10 | 0.022 | 0.022 | 0.019 | 0.013 |
| 15 | 0.015 | 0.015 | 0.013 | 0.009 |
| 20 | 0.011 | 0.011 | 0.010 | 0.006 |

Table 4 Equilibrium constant and thermodynamic parameters for the adsorption of CV onto PY adsorbent.

| [CV] ₀ (mg/L) | 5 | 10 | 15 | 20 | |
|----------------------------|--|-----------------------------------|----------------------------------|----------------------------------|-------|
| ΔG° (kJ/mol) | 293 K -10.16 303 K -10.86 313 K -11.39 323 K -12.20 | -7.64 -8.43 -9.70 -12.74 | -1.81 -2.18 -2.75 -3.61 | -1.26 -1.59 -2.01 -2.14 | |
| ΔH° (kJ/mol) | - | 9.28 | 40.57 | 15.52 | 7.72 |
| ΔS° (J/K mol) | - | 66.37 | 162.8 | 58.82 | 30.77 |

$$q_e = \frac{q_m K_L C_e}{1 + K_L C_e} \quad (6)$$

where q_m (mg/g) is the maximum adsorption capacity (monolayer coverage capacity), K_L (L/mg) is the equilibrium constant related to the affinity between adsorbent and adsorbate.

The essential characteristic of Langmuir isotherm can be expressed by the dimensionless constant called equilibrium parameter, R_L , defined by:

$$R_L = \frac{1}{1 + K_L C_0} \quad (7)$$

where R_L values indicate the type of isotherm to be irreversible ($R_L = 0$), favorable ($0 < R_L < 1$), and unfavorable ($R_L > 1$) (Mahmoodi and Arami, 2008).

The Freundlich isotherm (Freundlich, 1906) assumes that adsorption occurs over a heterogeneous surface with a multilayer adsorption mechanism, and that adsorbed amount increases with adsorbate concentration according to the following equation:

$$q_e = K_f C_e^{1/n} \quad (8)$$

where K_f ($\text{mg}^{1-1/n} \text{g}^{-1} \text{L}^{1/n}$) is the Freundlich constant and n is a constant related to adsorption intensity.

To compare the fitting quality of Langmuir and Freundlich isotherms in terms of the correlation coefficient R^2 , it was noticed that CV adsorption on the pyrophyllite is quite well consistent with Langmuir model but not with Freundlich one (Table 2). The dimensionless constant called equilibrium parameter which was calculated is grouped in Table 3. The results show that adsorption isotherms of CV on PY are all favorable. A similar result was obtained in recent studies such as Miyah et al. (2015). They found that the equilibrium adsorption data obtained for the CV adsorption on different adsorbents were well described by the Langmuir model.

3.8. Thermodynamics of adsorption

The thermodynamics' concept supposes that in an isolated system where energy cannot be gained or lost the thermodynamic parameters, which must be considered to determine the process, consist of changes in standard enthalpy (ΔH°), standard entropy (ΔS°) and free standard energy (ΔG°) due to the transfer of the body unit dissolved starting from the solution to the solid-liquid interface. The values of ΔH° and ΔS° were calculated using the following equation of Van't Hoff (El Haddad et al., 2013):

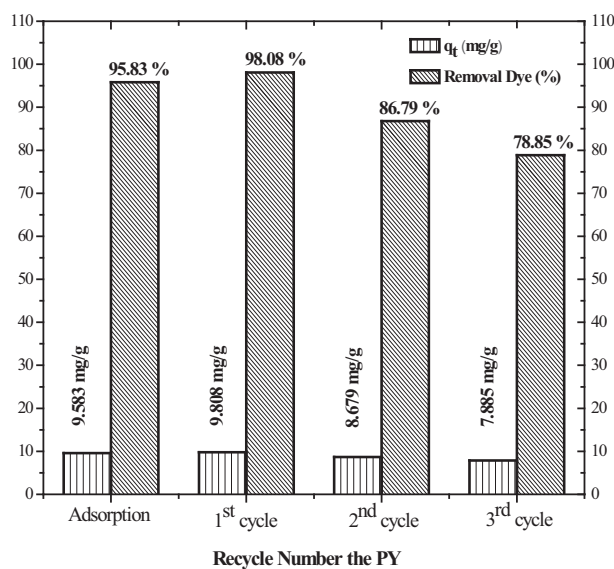
$$\ln K_d = \frac{\Delta S^\circ}{R} - \frac{\Delta H^\circ}{RT} \quad (9)$$

where R is the constant of perfect gas ($R = 8.314 \text{ J mol}^{-1} \text{ K}^{-1}$), T is the absolute temperature of solution (K), K_d is the partition coefficient.

The values of ΔH° and ΔS° were calculated starting from the slope and the interception of the layout of $\ln K_d$ according to $1/T$. ΔG° can be calculated below using the relation:

$$\Delta G^\circ = -RT \ln K_d \quad \text{and} \quad \Delta G^\circ = \Delta H^\circ - T\Delta S^\circ \quad (10)$$

ΔH° positive values show that the adsorption is endothermic process, while positive entropy ΔS° values reflect the increasing randomness at the solid/solution interface during

**Figure 9** Effect of regeneration cycle on the adsorption capacity and elimination percentage of CV.

the adsorption process (Mahmoodi et al., 2011). Negative values of free energy (ΔG°) at each temperature indicate the feasibility and spontaneity. The change in free energy ranged between -20 and 0 kJ/mol for physical reactions and between -400 and -80 kJ/mol for chemical reactions (El Haddad et al., 2013; Mahmoodi et al., 2011). ΔG° values in Table 4 are within -20 and 0 kJ/mol indicating that the physical reaction is a dominating mechanism.

Endothermic nature is also indicated by the increase in the adsorbed quantity with the increased temperature.

3.9. Regeneration of the pyrophyllite support

The economical and environmental aspects of used adsorbent materials, highlight the importance of the pyrophyllite reuse, considering their low cost and regeneration capacity.

The regeneration effect on the adsorption capacity of used pyrophyllite was studied by PY heat treatment at 500°C during 2 h after adsorption of Crystal Violet (10 mg/L). During tests of Crystal Violet adsorption, under the same operating conditions, described previously (Miyah et al., 2015) for a concentration of 10 mg/L, new adsorption capacities were obtained. These capacities are relatively important with those achieved at the beginning of the adsorption process (Fig. 9).

The difference in adsorption capacity and elimination percentage of CV compared to the first regeneration cycle is due to PY activation by a heat treatment. On the other hand, a light reduction of adsorption capacity was obtained after the second regeneration cycle of adsorbent studied; this was allowed by the reduction of specific PY surface following several heat treatments.

4. Conclusion

The present study shows that CV could be eliminated from aqueous solutions in eco-friendly conditions using PY adsorbent. It was demonstrated that the adsorbed quantity of dye increases with an increase of parameters such as temperature, pH solution, concentration and adsorbent amount. The decolorization percentage was 95.83%. Kinetic studies of dye on CV carried out the pseudo-second order at different dye concentration values. The Langmuir model describes satisfactory adsorption on the PY. Thermodynamic studies indicated that dye adsorption process by PY was spontaneous, physisorption and endothermic in nature. Finally, the increased regeneration cycles of pyrophyllite by a heat treatment decrease the adsorption quantity because of the decreased specific surface.

Conflict of interest

There is no conflict of interest.

References

- Almeida, C.A.P., Debacher, N.A., Downs, A.J., Cottet, L., Mello, C. A.D., 2009. Removal of methylene blue from colored effluents by adsorption on montmorillonite clay. *J. Colloid Interface Sci.* 332, 46–53.
- Barka, N., Qourzal, S., Assabbane, A., Nounah, A., Ait-Ichou, Y., 2011. Removal of reactive Yellow 84 from aqueous solutions by adsorption onto hydroxyapatite. *J. Saudi Chem. Soc.* 15, 263–267.
- El Haddad, M., Slimani, R., Mamouni, R., ElAntri, S., Lazar, S., 2013. Removal of two textile dyes from aqueous solutions onto calcined bones. *J. Assoc. Arab Univ. Basic Appl. Sci.* 14, 51–59.
- Ellouze, E., Tahri, N., Ben Amar, R., 2012. Enhancement of textile wastewater treatment process using nanofiltration. *Desalination* 286, 16–23.
- Freundlich, H.M.F., 1906. Über die adsorption in lösungen. *Zeitschrift für Physikalische Chemie (Leipzig)* 57A, 385–470.
- Guanghui, L., Jinghua, Z., Jun, L., Mingxia, L., Tao, J., Guanzhou, Q., 2014. Thermal transformation of pyrophyllite and alkali dissolution behavior of silicon. *Appl. Clay Sci.* 99, 282–288.
- Gupta, V.K., Suhas, 2009. Application of low-cost adsorbents for dye removal – a review. *J. Environ. Manage.* 90, 2313–2342.
- Güzel, F., Saygılı, H., Gülbahar, A.S., Filiz, K., 2015. New low-cost nanoporous carbonaceous adsorbent developed from carob (*Ceratonia siliqua*) processing industry waste for the adsorption of anionic textile dye: characterization, equilibrium and kinetic modeling. *J. Mol. Liq.* 206, 244–255.
- Haik, Y., Shahnaz, Q., Ashley, G., Sarmadia, A., Reyad, S., 2010. Phase change material for efficient removal of crystal violet dye. *J. Hazard. Mater.* 176, 1110–1112.
- Hao, O.J., Kim, H., Chiang, P.C., 2000. Decolorization of wastewater. *Crit. Rev. Env. Sci. Technol.* 30, 449–505.
- Idrissi, M., Miyah, Y., Chaouch, M., El Ouali Lalami, A., Lairini, S., Nenov, V., Zerrouq, F., 2014. CWPO du phenol, utilisant des catalyseurs à base de manganèse (CWPO of phenol Using manganese-based catalysts). *J. Mater. Environ. Sci.* 5, 2309–2313.
- Lagergren, S., 1898. About the theory of so-called adsorption of soluble substances. *Kungliga Svenska Vetenskapsakad. Handlingar* 24, 1–39.
- Langmuir, I., 1916. The constitution and fundamental properties of solids and liquids. Part I. solids. *J. Am. Chem. Soc.* 38, 2221–2295.
- Li, S.F., 2010. Removal of crystal violet from aqueous solution by sorption into semi interpenetrated networks hydrogels constituted of poly (acrylic acid–acrylamide–methacrylate) and amylase. *Bioreour. Technol.* 101, 2197–2202.
- Mahmoodi, N.M., Arami, M., 2008. Modelling and sensitivity analysis of dyes adsorption onto natural adsorbent from colored textile wastewater. *J. Appl. Polym. Sci.* 109, 4043–4048.
- Mahmoodi, N.M., Hayati, B., Arami, M., Lan, C., 2011. Adsorption of textile dyes on Pine Cone from colored wastewater: kinetic, equilibrium and thermodynamic studies. *Desalination* 268, 117–125.
- Mehmet, D., Karaoglu, M.H., Alkan, M., 2009. Adsorption kinetics of maxilon yellow 4GL and maxilon red GRL dyes on kaolinite. *J. Hazard. Mater.* 165, 1142–1151.
- Mittal, A., Mittal, J., Malviya, A., Kaur, D., Gupta, V.K., 2010. Adsorption of hazardous dye crystal violet from wastewater by waste materials. *J. Colloid Interface Sci.* 343, 463–473.
- Miyah, Y., Idrissi, M., Zerrouq, F., 2015. Study and modeling of the kinetics methylene blue adsorption on the clay adsorbents (pyrophyllite, calcite). *J. Mater. Environ. Sci.* 6 (3), 699–712.
- Mohamad Amran, M.S., Dalia, K.M., Wan, A.W.A.K., Azni, I., 2011. Cationic and anionic dye adsorption by agricultural solid wastes: a comprehensive review. *Desalination* 280, 1–13.
- Mustafa, T.Y., Tushar, K.S., Sharmeen, A., Ang, H.M., 2014. Dye and its removal from aqueous solution by adsorption: a review. *Adv. Colloid Interface Sci.* 209, 172–184.
- Njoku, V.O., Foo, K.Y., Asif, M., Hameed, B.H., 2014. Preparation of activated carbons from rambutan (*Nephelium lappaceum*) peel by microwave-induced KOH activation for acid yellow 17 dye adsorption. *Chem. Eng. J.* 250, 198–204.
- Ollis, D., Silva, C.G., Faria, J., 2015. Simultaneous photochemical and photocatalyzed liquid phase reactions: dye decolorization kinetics. *Catal. Today* 240, 80–85.

- Ru-Ling, T., Pin-Hsueh, W., Feng-Chin, W., Ruey-Shin, J., 2014. A convenient method to determine kinetic parameters of adsorption processes by nonlinear regression of pseudo- n th-order equation. *Chem. Eng. J.* 237, 153–161.
- Sheng, J., Xie, Y., Zhou, Y., 2009. Adsorption of methylene blue from aqueous solution on pyrophyllite. *Appl. Clay Sci.* 46, 422–424.
- Singh, K.P., Shikha, G., Arun, K.S., Sarita, S., 2011. Optimizing adsorption of crystal violet dye from water by magnetic nanocomposite using response surface modeling approach. *J. Hazard. Mater.* 186, 462–473.
- Sivashankar, R., Sathya, A.B., Vasantharaj, K., Sivasubramanian, V., 2014. Magnetic composite an environmental super adsorbent for dye sequestration – a review. *Environ. Nanotechnol. Monit. Manage.* 1–2, 36–49.
- Talal, S., 2014. Sorption kinetics: obtaining a pseudo-second order rate equation based on a mass balance approach. *J. Environ. Chem. Eng.* 2, 1001–1006.
- Weber, W.J., Morris, J.C., 1963. Kinetics of Adsorption on Carbon from Solution. *J. Sanit. Eng. Div. Am. Soc. Civil Eng.* 89, 31–59.
- Weng, C.H., Pan, Y.F., 2007. Adsorption of a cationic dye (methylene blue) onto spent activated clay. *J. Hazard. Mater.* 144, 355–362.
- Wojciech, K., Krzysztof, C., Grzegorz, B., Ewa, M., 2015. Study on efficient removal of anionic, cationic and nonionic dyes from aqueous solutions by means of mesoporous carbon nanospheres with empty cavity. *Chem. Eng. Res. Des.* 94, 242–253.
- Zhang, J., Yan, J., Sheng, J., 2015. Dry grinding effect on pyrophyllite–quartz natural mixture and its influence on the structural alternation of pyrophyllite. *Micron* 71, 1–6.
- Zhiguo, P., Shuang, Y., Lingyun, L., Chunmei, L., Shuzhen, Z., Xiaoquan, S., Bei, W., Baoyuan, G., 2014. Effects of copper and aluminum on the adsorption of sulfathiazole and tylosin on peat and soil. *Environ. Pollut.* 184, 579–585.